

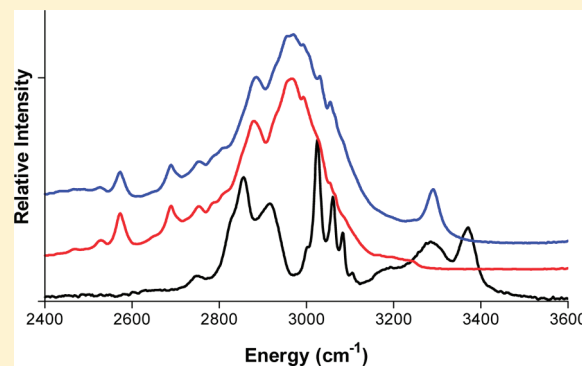
Vibrational Spectroscopic Studies of Cocrystals and Salts.

4. Cocrystal Products formed by Benzylamine, α -Methylbenzylamine, and their Chloride Salts

Harry G. Brittain*

Center for Pharmaceutical Physics, 10 Charles Road Milford, New Jersey 08848, United States

ABSTRACT: The chloride salts formed by benzylamine and α -methylbenzylamine have been characterized using X-ray powder diffraction, differential scanning calorimetry, and infrared absorption spectroscopy. In addition, X-ray powder diffraction and differential scanning calorimetry have been used to establish formation or lack of formation of the 1:1 stoichiometric salt-cocrystal products containing the chloride salts and their respective free bases. For α -methylbenzylamine (which contains a single dissymmetric center), the chiral identities of the free bases and chloride salts were found to play a determining role as to whether a salt-cocrystal product could or could not be formed. It was found that a salt-cocrystal product could only be formed if the salt and free base were of opposite absolute configurations. For those systems where the existence of cocrystals was demonstrated, assignments were derived for the observed peaks in the infrared absorption spectra of the reactants and their products.



INTRODUCTION

As the science of crystal engineering continues to yield new supramolecular synthons capable of being assembled into an ever-widening sphere of crystalline solids, the scope of suitable intermolecular interactions continues to grow. Schultheiss and Newman¹ have summarized six definitions of a cocrystal that go beyond the definition of Aakeröy, who had proposed that a cocrystal is a homogeneous crystalline solid that contains stoichiometric amounts of discrete neutral molecular species that are solids under ambient conditions.² Part of the expansion in scope reflects developments in cocrystals having pharmaceutical interest, and where the drug substance is present in an ionic form.^{3–5} The question of whether a given species is a cocrystal or a salt has been addressed, considering the effect of the overall crystal structure on the ionization state and degree of proton transfer in such species.^{6,7}

One area of cocrystal research that has not received a great deal of attention concerns the systems where salts of organic molecules form cocrystals with the neutral organic molecule from which the salt was made. For example, the existence of a salt-cocrystal product formed by the cocrystallization of tiotropium fumarate with fumaric acid has been demonstrated and shown to be more stable than either the salt or salt-solvate solid forms.⁸ In this laboratory, vibrational spectroscopy has been used to study intermolecular interactions in the 1:1 salt-cocrystal formed by the interaction of benzoic acid with benzylammonium benzoate,⁹ as well as the salt-cocrystal products formed by a series of benzenecarboxylic acids and their sodium salts.¹⁰

Whereas the aforementioned studies investigated the phenomenon of salt-cocrystal formation among acidic substances

and their salts, the present study is concerned with the formation of salt-cocrystal products resulting from the interaction of basic substances with their corresponding acid addition salts. Thus, the present study relates to the scope of intermolecular interactions existing in these systems containing different modes of anion coordination and anion-templated assemblies.¹¹

The present work investigates the salt-cocrystal systems formed by benzylamine and α -methylbenzylamine with their corresponding chloride salts. The formation of a particular salt-cocrystal product (or the absence of its formation) was demonstrated by means of X-ray powder diffraction and differential scanning calorimetry. Subsequently, trends in the energies of molecular vibrations were used to deduce selection rules that could be more generally used as additional tools for the identification and characterization of salt-cocrystal species.

It has been demonstrated for the first time that stereoselectivity can exist in the formation of salt-cocrystal products when the interacting species contain centers of dissymmetry. In particular, it has been found that a salt-cocrystal product could be formed if the salt and free base were of opposite absolute configurations, but that no cocrystallization would take place if the salt and free base were of the same absolute configuration.

MATERIALS AND METHODS

Benzylamine, (*R*)- and (*S*)- α -methylbenzylamine were obtained from Aldrich and were used as received. The chloride salts of these

Received: March 1, 2011

Revised: April 15, 2011

Published: April 19, 2011

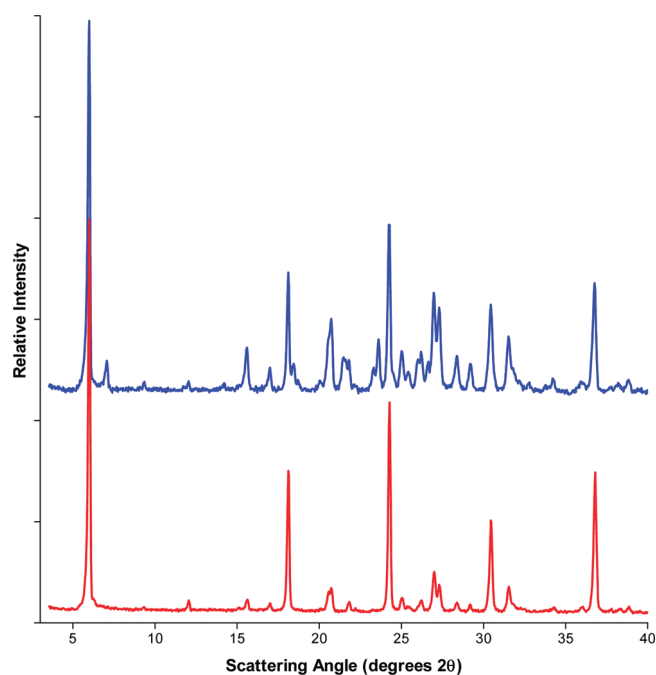


Figure 1. X-ray powder diffraction patterns of benzylammonium chloride (red trace) and the 1:1 benzylamine/benzylammonium chloride salt-cocrystal (blue trace).

phenylalkylamines were prepared by dissolving approximately 250 mg quantities in 10 mL of methanol, to which was added a 1:1 stoichiometric amount of 2.0 N hydrochloric acid (obtained from Spectrum Chemicals). The solutions were allowed to evaporate to dryness, whereupon the recovered solids were transferred to a mortar, wetted with methanol, and ground until solid. Salt-cocrystal products were prepared using the wet-grinding method, where accurately weighed equimolar amounts of free amine and chloride salt were placed in a mortar, ground to create homogeneity in the mix, wetted with two drops of methanol, and then the mixture was ground until dry. As will be discussed below, the process was usually completed fairly rapidly, but in a few instances the mixtures required a long period of time to become fully dry.

X-ray powder diffraction (XRPD) patterns were obtained using a Rigaku MiniFlex powder diffraction system (X-ray source being nickel-filtered $K\alpha$ emission of copper), equipped with a horizontal goniometer operating in the $\theta/2\theta$ mode. Samples were packed into the sample holder using a backfill procedure and were scanned over the range of 3.5–40 deg 2θ at a scan rate of 0.5 degrees 2θ /min. Using a data acquisition rate of 1 point per second, these scanning parameters equate to a step size of 0.0084 degrees 2θ .

Measurements of differential scanning calorimetry (DSC) were obtained on a TA Instruments 2910 thermal analysis system. Samples of approximately 1–2 mg were accurately weighed into an aluminum DSC pan and then covered with an aluminum lid that was crimped in place. Samples were heated at a rate of 10 °C/min from ambient temperature to termination temperatures in the range of 150 to 225 °C, depending on the system under study. Thermally induced weight loss measurements were performed using an Ohaus MB-45 moisture balance.

Fourier-transform infrared (FTIR) absorption spectra were obtained at a resolution of 2 cm^{-1} using a Shimadzu model 8400S infrared spectrometer, with each spectrum being obtained as the average of 25 individual spectra. The data were acquired using the attenuated total reflectance sampling mode, where the samples were clamped against the ZnSe crystal of a Pike MIRacle single reflection horizontal ATR sampling accessory.

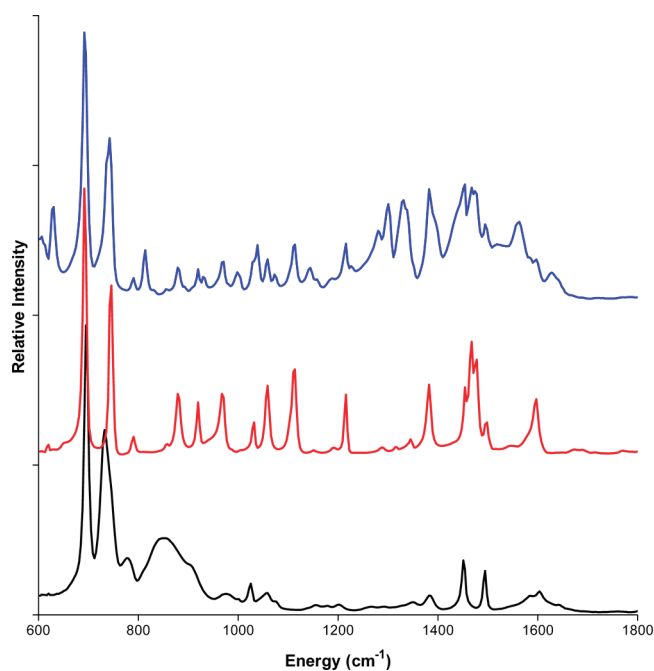
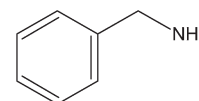


Figure 2. Infrared absorption spectra in the fingerprint region of benzylamine (black trace), benzylammonium chloride (red trace), and the 1:1 benzylamine/benzylammonium chloride salt-cocrystal (blue trace).

RESULTS AND DISCUSSION

A. Benzylamine, Benzylammonium Chloride, and their Salt-Cocrystal Product. The interaction of benzylamine (BZA):



with benzylammonium chloride was the first system to be investigated. During the solvent-drop grinding process used, no odor of benzylamine could be detected, and the ground solids were found to dry down to a powdered solid in less than 30 min. This observation was taken as an initial indication of the formation of a salt-cocrystal product.

Since benzylamine is a liquid at room temperature, its XRPD pattern could not be obtained. The benzylammonium chloride (BZA-Cl) salt and the benzylamine–benzylammonium chloride (BZA-Cl-BZA) salt-cocrystal were both obtained in solid form, so their respective XRPD patterns are shown in Figure 1. Although the two diffraction patterns are somewhat similar in appearance, the formation of a BZA-Cl-BZA salt-cocrystal product was confirmed by the presence of additional diffraction peaks in its powder pattern.

The DSC thermograms obtained for the solid products confirmed that a salt-cocrystal product was produced by the interaction between benzylamine and benzylammonium chloride. The DSC thermogram of the BZA-Cl salt demonstrated this product to be nonsolvated, as the thermogram contained only a single thermally induced endothermic transition. Owing to its high temperature (maximum at 200 °C; enthalpy of fusion equal to 34 J/g), this event was assigned to melting of the salt. The BZA-Cl-BZA salt-cocrystal was also found to be nonsolvated,

Table 1. Assignments of the Major Bands in the Fingerprint Region of the Infrared Absorption Spectra of Benzylamine, Benzylammonium chloride, and Their 1:1 Salt-Cocrystal Product

free base vibrational mode assignment	benzylamine	BZA-Cl-BZA salt-cocrystal	benzyl-ammonium chloride	chloride salt vibrational mode assignment
in-plane ring deformation mode		629	619	in-plane ring deformation mode
C–H out-of-plane deformation mode	696	692	692	C–H out-of-plane deformation mode
C–H out-of-plane phase deformation mode	733	743	744	C–H out-of-plane phase deformation mode
out-of-plane ring deformation mode	777	791	791	out-of-plane ring deformation mode
		814		
NH ₂ out-of-plane bending mode	851			
		879	879	NH ₃ ⁺ out-of-plane bending mode
		920	920	CH ₂ rocking mode
		932		
C–C stretching mode	974	970	968	C–C stretching mode
		999		
in-plane C–H deformation mode	1024	1030	1032	in-plane C–H deformation mode
		1040		
in-plane C–H deformation mode	1059	1059	1059	in-plane C–H deformation mode
		1074		
		1113	1113	in-plane C–H deformation mode
NH ₂ rocking mode	1155	1144		
in-plane C–H deformation mode	1178	1188	1190	in-plane C–H deformation mode
in-plane C–H deformation mode	1202	1215	1215	in-plane C–H deformation mode
NH ₂ rocking mode	1267			
		1283		
		1302		
		1331	1315	NH ₃ ⁺ rocking mode
C–N stretching mode	1350	1346	1346	C–N stretching mode
C–C ring stretching mode	1385	1383	1383	C–C ring stretching mode
C–C ring stretching mode	1452	1454	1454	C–C ring stretching mode
		1468	1466	CH ₂ deformation mode
		1475	1477	CH ₂ deformation mode
C–C ring stretching mode	1495	1497	1497	C–C ring stretching mode
		1562		
C–C ring stretching mode	1589	1585		C–C ring stretching mode
C–C ring stretching mode	1605	1597	1597	C–C ring stretching mode
		1628		NH ₃ ⁺ symmetric bending mode

exhibiting a melting endothermic transition at a temperature of 132 °C with an enthalpy of fusion equal to 48 J/g.

As shown in Figure 2, benzylamine, benzylammonium chloride, and the BZA-Cl-BZA salt-cocrystal exhibited several significant differences in the fingerprint region of their FTIR spectra that are consistent with formation of the salt-cocrystal product. In order to fully interpret the spectra, the molecular vibrational modes of the major absorbance bands of benzylamine and benzylammonium chloride were assigned through the use of published compilations^{12–15} and works conducted specifically on phenylalkylamines and their derivatives.^{16–25} Assignments for the absorption bands of the salt-cocrystal were made whenever possible by extrapolation. The results of this analysis are provided in Table 1.

In general, the energies of the carbon–carbon ring modes and the carbon–hydrogen deformation modes were comparable for the three substances, indicating that the motions associated with the basic organic skeleton were effectively equivalent. Not surprisingly, the most important differences between the spectra

of the free amine and its chloride salt were associated with the amine group and its protonation. The most important change associated with salt formation was the loss of the broad absorption band associated with the free amine –NH₂ out-of-plane bending mode at 851 cm^{–1} and the appearance of the relatively sharp –NH₃⁺ out-of-plane bending mode at 879 cm^{–1}. In addition, the pair of free amine –NH₂ rocking modes at 1155 and 1267 cm^{–1} were lost upon formation of the chloride salt, and the –NH₃⁺ rocking mode was observed at 1315 cm^{–1}.

The formation of the BZA-Cl-BZA salt-cocrystal led to additional perturbations in the fingerprint region of its FTIR spectrum. Although the –NH₃⁺ out-of-plane bending mode was observed at 879 cm^{–1} (the same as for the chloride salt), perturbed –NH₂ rocking modes were evident at 1144 and 1283 cm^{–1}. In addition, the –NH₃⁺ rocking mode of the salt underwent a shift to 1331 cm^{–1}. It was interesting to note the appearance of new absorption bands at 932, 999, 1074, 1302, and 1562 cm^{–1} whose origin could not be deduced from knowledge of the assignments of either the free base or chloride salt. Perhaps

most significant is the appearance of the -NH_3^+ symmetric bending mode (1628 cm^{-1}) in the spectrum of the BZA-Cl-BZA salt-cocrystal which was not observed in the spectrum of the hydrochloride salt.

However, as shown in Figure 3, the phenomena of salt formation was most evident in the high-frequency region of the FTIR spectrum (a full summary of the peak assignments is found in Table 2). For the free amine, the aliphatic $\text{-CH}_2\text{-}$ symmetric and antisymmetric stretching modes are observed at 2856 and 2916 cm^{-1} , respectively, while the aromatic -CH stretching modes are found at 3026 , 3061 , and 3084 cm^{-1} .

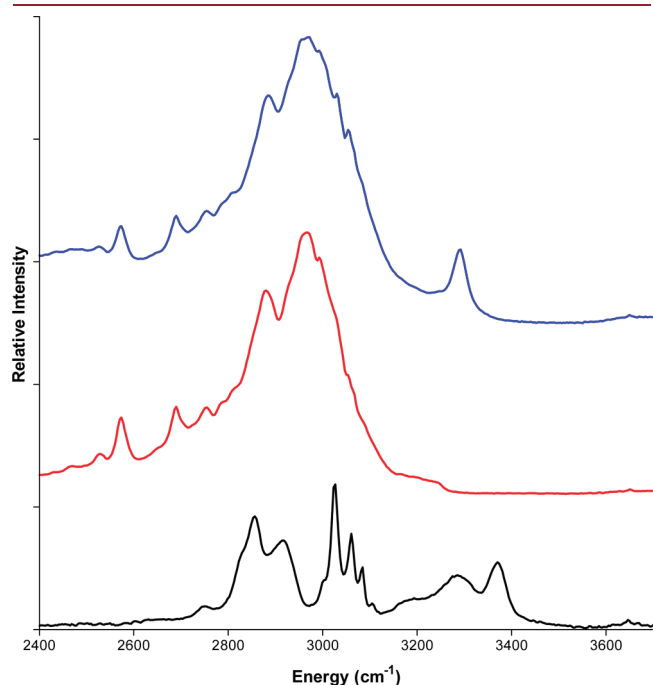
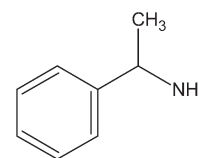


Figure 3. Infrared absorption spectra in the high-frequency region of benzylamine (black trace), benzylammonium chloride (red trace), and the 1:1 benzylamine/benzylammonium chloride salt-cocrystal (blue trace).

Formation of the benzylammonium chloride salt from benzylamine was most evident by the disappearance of the antisymmetric and symmetric stretching bands associated with the -NH_2 group (3285 and 3371 cm^{-1} , respectively). Upon formation of the salt, the antisymmetric and symmetric stretching bands of the -NH_3^+ group shift to lower energy, and one observed a rather broad absorption around 2965 cm^{-1} that represents an overlapping system with the aromatic -CH stretching modes. One of the aliphatic $\text{-CH}_2\text{-}$ stretching modes shifted to 2880 cm^{-1} upon salt formation, and overtones of -NH_3^+ deformation modes not observed in the spectrum of the free amine become evident as absorption bands at 2573 , 2691 , and 2754 cm^{-1} .

As evident in Figure 3, the high-frequency FTIR spectrum of the BZA-Cl-BZA salt-cocrystal resembled that of the benzylammonium chloride salt. The broad band formed by the overlap of the -NH_3^+ antisymmetric and symmetric stretching bands with the aromatic -CH stretching modes was now observed as a broad band around 2970 cm^{-1} , the aliphatic $\text{-CH}_2\text{-}$ stretching modes shifted to 2885 cm^{-1} , and the -NH_3^+ overtone modes were observed at 2573 , 2691 , and 2754 cm^{-1} . Most significant, however, is the appearance of a new absorption band at 3290 cm^{-1} in the spectrum of the BZA-Cl-BZA salt-cocrystal, which has been assigned as one of the -NH_3^+ stretching modes.

B. α -Methylbenzylamine, α -Methylbenzylammonium Chloride, and their Salt-Cocrystal Products. The α -methylbenzylamine (mBZA) system:



adds an interesting complication in that the compound contains one center of dissymmetry and is therefore capable of existing as a racemic mixture or as separated enantiomers. This stereochemistry therefore presents an opportunity to examine any possible stereoselectivity in the salt-cocrystal formation, since the choice of enantiomeric identities of the amine and salt precursors, and

Table 2. Assignments of the Major Bands in the High-Frequency Region of the Infrared Absorption Spectra of Benzylamine, Benzylammonium chloride, and their 1:1 Salt-Cocrystal Product

free base vibrational mode assignment	benzylamine	BZA-Cl-BZA salt-cocrystal	benzyl-ammonium chloride	chloride salt vibrational mode assignment
		2573	2573	overtone band
		2691	2691	overtone band
		2754	2754	overtone band
symmetric CH_2 stretching mode	2856			
		2885	2880	aliphatic CH_2 stretching mode
antisymmetric CH_2 stretching mode	2916			
		2970	2965	composite band
aromatic CH stretching mode	3026	3030		
aromatic CH stretching mode	3061	3055	3053	aromatic CH stretching mode
aromatic CH stretching mode	3084			
		3290 (NH_3^+ stretching mode)		
NH_2 symmetric stretching mode	3285			
NH_2 antisymmetric stretching mode	3371			

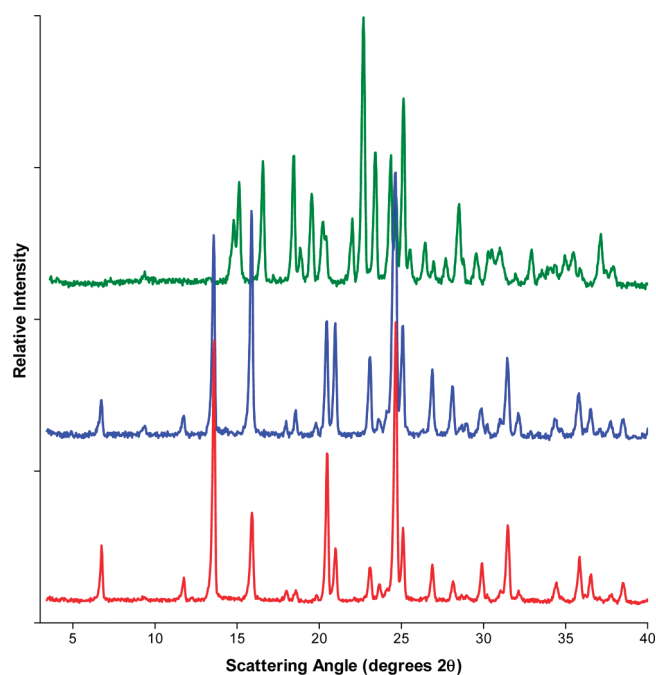


Figure 4. X-ray powder diffraction patterns of (*R*)- α -methylbenzylammonium chloride (red trace), and the (*R*)mBZA-Cl-(*R*)mBZA (blue trace) and (*R*)mBZA-Cl-(*S*)mBZA (green trace) salt-cocrystal products.

the consequent presence of two centers of dissymmetry in a salt-cocrystal product, could result in homodiastereomer and heterodiastereomer products.

The existence of stereoselectivity became apparent during the solvent-drop grinding process used to promote the interaction between enantiomeric resolved α -methylbenzylamine and α -methylbenzylammonium chloride precursors. No amine odor was detected during the grinding of (*R*)- α -methylbenzylamine with (*S*)- α -methylbenzylammonium chloride, or during the grinding of (*S*)- α -methylbenzylamine with (*R*)- α -methylbenzylammonium chloride indicating incorporation of the phenylalkylamine into a salt-cocrystal product. These ground solids were found to yield a dry powdered solid in less than 30 min. On the other hand, a strong phenylalkylamine odor was noted during the grinding of (*R*)- α -methylbenzylamine with (*R*)- α -methylbenzylammonium chloride, and during the grinding of (*R*)- α -methylbenzylamine with (*R*)- α -methylbenzylammonium chloride. That the products of these interactions required overnight periods to fully dry down to a powdered solid is strongly suggestive that a salt-cocrystal product was not formed during these solvent-drop grinding processes.

Since the (*R*) and (*S*) forms of α -methylbenzylamine are all liquids at room temperature, their XRPD patterns could not be obtained, and the (*R*) and (*S*) enantiomerically pure forms of α -methylbenzylammonium chloride exhibited identical XRPD patterns. The XRPD patterns obtained for the (*R*)mBZA-Cl salt are found in Figure 4, along with the patterns of the (*R*)mBZA-Cl-(*R*)mBZA and (*R*)mBZA-Cl-(*S*)mBZA salt-cocrystal products. The XRPD pattern of the (*R*)mBZA-Cl-(*S*)mBZA salt-cocrystal product was found to contain a sufficient number of distinctions relative to the chloride salt so as to confirm the formation of a salt-cocrystal product.

On the other hand, aside from some small differences in relative intensity, the XRPD patterns of (*R*)mBZA-Cl and the

(*R*)mBZA-Cl-(*R*)mBZA salt-cocrystal product were effectively the same. This finding strongly suggests that a salt-cocrystal product could not be formed during the solvent-drop grinding process, and the olfactory observation of phenylalkylamine odor indicates that the free amine simply volatilized during the grinding process. In the absence of a mechanism to incorporate the phenylalkylamine into a suitable solid-state structure, the final product of the attempted interaction would simply be the residual chloride salt precursor.

These results confirm the existence of stereoselectivity in formation of α -methylbenzylamine salt-cocrystal products, since only the interaction of (*R*)mBZA-Cl and (*S*)mBZA formed the anticipated salt-cocrystal product, and the attempted interaction of (*R*)mBZA-Cl and (*R*)mBZA yielded only the (*R*)mBZA-Cl salt.

The trends noted in the XRPD patterns of the α -methylbenzylamine products were confirmed in their thermal analysis profiles. None of the salts or salt-cocrystal products exhibited an endothermic transition at low temperatures and were therefore determined to be nonsolvated in nature. In its thermogram, the (*R*)mBZA-Cl-(*S*)mBZA salt-cocrystal product exhibited a melting endothermic transition characterized by a lower temperature (maximum at 159 °C) and a significantly higher enthalpy of fusion (equal to 124 J/g) when compared to the analogous features observed for relative to (*R*)mBZA-Cl salt (i.e., temperature maximum of 171 °C and enthalpy of fusion equal to 75 J/g).

On the other hand, the melting endotherm obtained for the product obtained by the attempted interaction of (*R*)mBZA-Cl and (*R*)mBZA was found to be equivalent to that of the (*R*)mBZA-Cl salt within experimental error (i.e., temperature maximum at 172 °C and enthalpy of fusion equal to 79 J/g). The DSC results therefore confirm the formation of a (*R*)mBZA-Cl-(*S*)mBZA salt-cocrystal product and the nonexistence of a (*R*)mBZA-Cl-(*R*)mBZA salt-cocrystal product.

The trends associated with the peaks in the fingerprint region within the FTIR spectra of (*R*)mBZA, the (*R*)mBZA-Cl salt, and the (*R*)mBZA-Cl-(*S*)mBZA salt-cocrystal product may be observed in the spectra shown in Figure 4. The existence of stereoselectivity in the formation of salt-cocrystal products was again demonstrated, since the spectrum of the (*R*)mBZA-Cl-(*R*)mBZA product was effectively the same as that of the (*R*)mBZA-Cl salt. The FTIR spectrum of the (*R*)mBZA-Cl-(*S*)mBZA product was unique, confirming the existence of the salt-cocrystal product.

The vibrational origins of the major absorbance bands observed in the various FTIR spectra were derived as before, namely, using published compilations^{12–15} and works conducted specifically on phenylalkylamines and their derivatives^{16–25} to obtain the assignments collected in Table 3. As noted with the benzylamine series, the most important effects evident in the spectra were associated with the protonation of the free amine to yield the chloride salt. The free amine $-\text{NH}_2$ out-of-plane bending mode at 841 cm^{-1} and the two free amine $-\text{NH}_2$ rocking modes at 1155 and 1279 cm^{-1} were lost upon formation of the chloride salt, being replaced by a sharp peak at 879 cm^{-1} derived from the $-\text{NH}_3^+$ out-of-plane bending mode and the $-\text{NH}_3^+$ rocking mode at 1317 cm^{-1} , respectively. Finally, the $-\text{NH}_3^+$ symmetric bending mode was observed at 1620 cm^{-1} in the spectrum of the chloride salt.

The formation of the (*R*)mBZA-Cl-(*S*)mBZA salt-cocrystal caused the appearance of additional perturbations in the fingerprint region of its FTIR spectrum. The $-\text{NH}_3^+$ out-of-plane bending mode shifted to 895 cm^{-1} , and the $-\text{NH}_3^+$ rocking

Table 3. Assignments of the Major Bands in the Fingerprint Region of the Infrared Absorption Spectra of (*R*)- α -Methylbenzylamine, (*R*)- α -Methylbenzylammonium chloride, and the two Diastereomeric 1:1 Salt-Cocrystal Products

free base vibrational mode assignment	(<i>R</i>)- α -methylbenzyl-amine	(<i>R</i>)mBZA-Cl-(<i>S</i>)mBZA salt-cocrystal	(<i>R</i>)mBZA-Cl-(<i>R</i>)mBZA salt-cocrystal	(<i>R</i>)- α -methylbenzyl-ammonium chloride	chloride salt vibrational mode assignment
C–H out-of-plane deformation mode	698	696	696	696	C–H out-of-plane deformation mode
C–H out-of-plane phase deformation mode		752	748	748	C–H out-of-plane phase deformation mode
out-of-plane ring deformation mode	762	766	762	762	out-of-plane ring deformation mode
		812			
NH ₂ out-of-plane bending mode	841				
		895	881	879	NH ₃ ⁺ out-of-plane bending mode
		905			
CH ₂ rocking mode	912	916	912	914	CH ₂ rocking mode
C–C stretching mode	997	996	991	991	C–C stretching mode
		1001	1003	1003	C–C stretching mode
in-plane C–H deformation mode	1022	1026	1018	1019	in-plane C–H deformation mode
in-plane C–H deformation mode			1032	1032	in-plane C–H deformation mode
in-plane C–H deformation mode	1055	1053	1067	1067	in-plane C–H deformation mode
in-plane C–H deformation mode	1105	1111	1134	1132	in-plane C–H deformation mode
		1151			
NH ₂ rocking mode	1155				
in-plane C–H deformation mode	1184	1186	1176	1176	in-plane C–H deformation mode
in-plane C–H deformation mode	1236	1232	1229	1229	in-plane C–H deformation mode
NH ₂ rocking mode	1279				
CH ₃ deformation mode	1292	1290	1292	1292	CH ₃ deformation mode
		1315	1317	1317	NH ₃ ⁺ rocking mode
C–N stretching mode	1329	1333	1333	1337	C–N stretching mode
CH ₃ symmetric deformation mode	1367	1371	1383	1383	CH ₃ symmetric deformation mode
		1387	1393	1393	C–C ring stretching mode
C–C ring stretching mode	1450	1452	1452	1454	C–C ring stretching mode
C–C ring stretching mode	1491	1495	1497	1497	C–C ring stretching mode
		1514			
		1549			
C–C ring stretching mode	1585	1585			C–C ring stretching mode
C–C ring stretching mode	1603	1599	1601	1601	C–C ring stretching mode
		1610	1622	1620	NH ₃ ⁺ symmetric bending mode

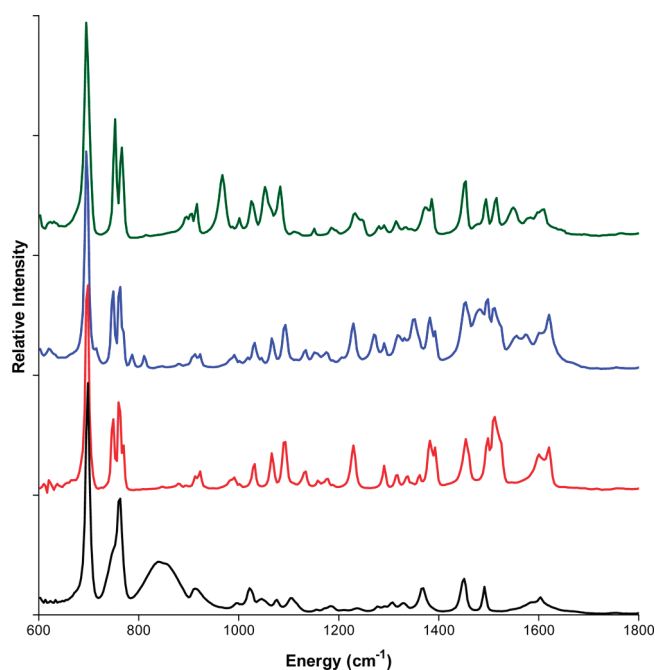
mode of the salt underwent a slight shift to 1315 cm⁻¹. Unlike the BZA-Cl-BZA salt-cocrystal where perturbed –NH₂ rocking mode bands could be observed in the spectrum, no such bands were evident in the spectrum of the (*R*)mBZA-Cl-(*S*)mBZA salt-cocrystal. Only four new absorption bands (at 812, 905, 1514, and 1549 cm⁻¹) were observed which could not be assigned on the basis of assignments pertaining to either the free base or the

chloride salt. For the (*R*)mBZA-Cl-(*S*)mBZA salt-cocrystal, the –NH₃⁺ symmetric bending mode was found to undergo a modest shift down to 1628 cm⁻¹.

As shown in Figure 3 and summarized in Table 4, the phenomena of salt formation was again highly visible in the high-frequency region of the FTIR spectrum. Formation of the α -methylbenzylammonium chloride salt was demonstrated

Table 4. Assignments of the Major Bands in the High-Frequency Region of the Infrared Absorption Spectra of (*R*)- α -Methylbenzylamine, (*R*)- α -Methylbenzylammonium chloride, and the two Diastereomeric 1:1 Salt-Cocrystal Products

free base vibrational mode assignment	(<i>R</i>)-(methylbenzyl-amine	(<i>R</i>)mBZA-Cl-(<i>S</i>)mBZA salt-cocrystal	(<i>R</i>)mBZA-Cl-(<i>R</i>)mBZA salt-cocrystal	(<i>R</i>)-(methylbenzyl-ammonium chloride	chloride salt vibrational mode assignment
		2505	2494	2494	overtone band
		2573	2588	2584	overtone band
		2617	2635	2635	overtone band
		2691	2685	2685	overtone band
		2735	2737	2739	overtone band
symmetric CH ₂ stretch	2866				
		2887	2887	2885	aliphatic CH ₂ stretch
antisymmetric CH ₂ stretch	2924	2920			
			2956	2955	composite band
aliphatic CH ₃ stretch	2961	2965			
aromatic CH	3024	2972			
aromatic CH	3061	3034			
aromatic CH	3082	3063			
		3248 (antisymmetric NH ₃ ⁺ stretch)			
antisymmetric NH ₂ stretch	3288	3292 (symmetric NH ₃ ⁺ stretch)			
symmetric NH ₂ stretch	3366				

**Figure 5.** Infrared absorption spectra in the fingerprint region of (*R*)- α -methylbenzylamine (black trace), (*R*)- α -methylbenzylammonium chloride (red trace), and the (*R*)mBZA-Cl-(*R*)mBZA (blue trace) and (*R*)mBZA-Cl-(*S*)mBZA (green trace) salt-cocrystal products.

by the disappearance of the antisymmetric and symmetric stretching bands associated with the $-\text{NH}_2$ group (3288 and 3366 cm^{-1} , respectively). Upon formation of the salt, the absorption bands of the $-\text{NH}_3^+$ stretching modes were found

to merge into absorption bands associated with the aromatic $-\text{CH}$ stretching modes, resulting in a broad absorption band around 2955 cm^{-1} . A large number of overtone bands not observed in the spectrum of the free amine were observed at energies of 2494, 2584, 2635, 2685, and 2739 cm^{-1} .

Once again, the pattern of high-frequency absorption bands associated with the (*R*)mBZA-Cl-(*R*)mBZA product and the (*R*)mBZA-Cl salt could not be distinguished, which is consistent with the lack of formation of a salt-cocrystal product. However, formation of the (*R*)mBZA-Cl-(*S*)mBZA salt-cocrystal product was amply demonstrated by the presence of absorption bands associated with the perturbed symmetric (3292 cm^{-1}) and antisymmetric (3248 cm^{-1}) $-\text{NH}_3^+$ stretching modes.

C. Formation of Mixed Salt-Cocrystal Products. The demonstrated stereoselectivity associated with the α -methylbenzylamine system indicated that a study of possible mixed salt-cocrystal products would be of interest. In a previous study, it was found that mixed salt-cocrystal products could be formed by the solvent-drop grinding of a benzenecarboxylic acid with the sodium salt of a different benzenecarboxylic acid.¹⁰ To learn whether a similar interaction could take place between the benzylamines of the present investigation, a study of the interaction of (*R*)- α -methylbenzylamine with benzylammonium chloride and a study of the interaction of (*R*)- α -methylbenzylammonium chloride with benzylamine was undertaken.

The XRPD patterns obtained for the BZA-Cl and (*R*)mBZA-Cl salts are found in Figure 7 together with the pattern of the (*R*)mBZA-Cl-BZA salt-cocrystal product that had been prepared by the interaction of (*R*)- α -methylbenzylamine with benzylammonium chloride. It was found that while the diffraction pattern of the salt-cocrystal product contained a number of scattering peaks in common with the XRPD of BZA-Cl, a sufficient number of differences were observed that indicated

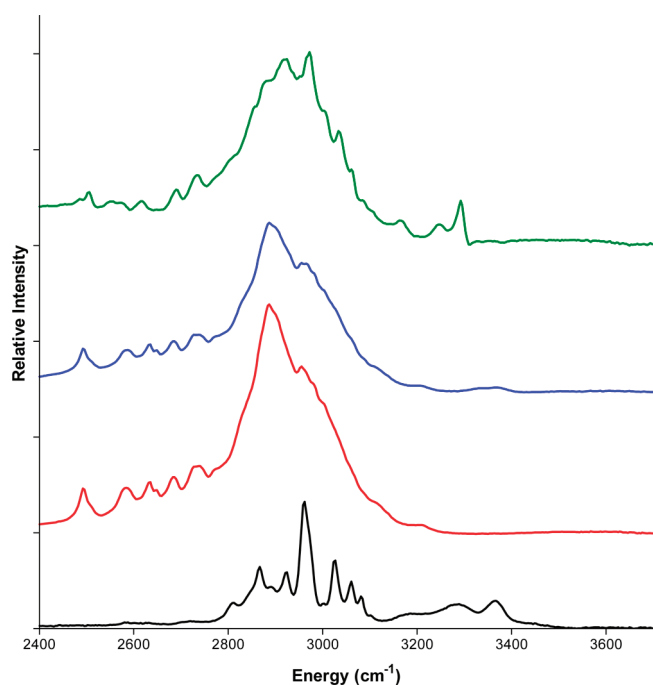


Figure 6. Infrared absorption spectra in the high-frequency region of (*R*)- α -methylbenzylamine (black trace), (*R*)- α -methylbenzylammonium chloride (red trace), and the (*R*)mBZA-Cl-(*R*)mBZA (blue trace) and (*R*)mBZA-Cl-(*S*)mBZA (green trace) salt-cocrystal products.

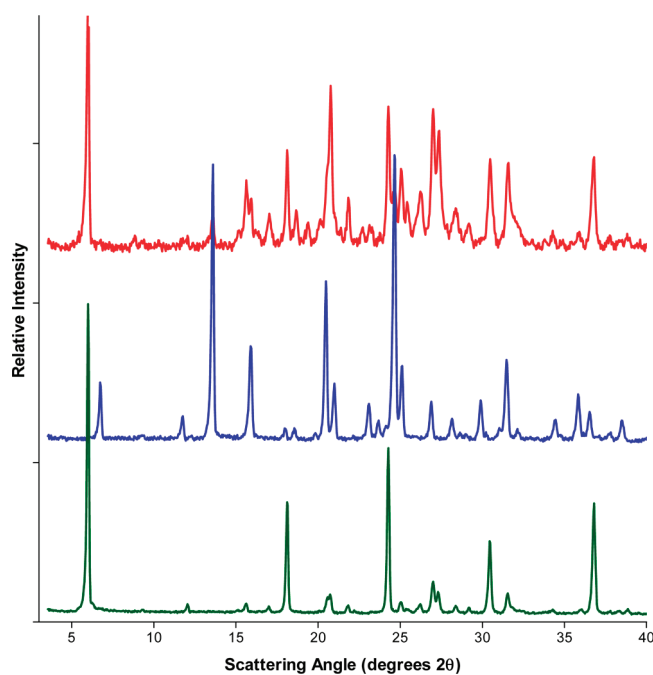


Figure 7. X-ray powder diffraction patterns of benzylammonium chloride (green trace), (*R*)- α -methylbenzylammonium chloride (blue trace), and their 1:1 cocrystal product (red trace).

the formation of a new crystalline species. Although not shown in the figure, the XRPD pattern of the salt-cocrystal product formed by the interaction of benzylamine with (*R*)- α -methylbenzylammonium chloride was equivalent to the XRPD of the salt-cocrystal product that had been prepared by the

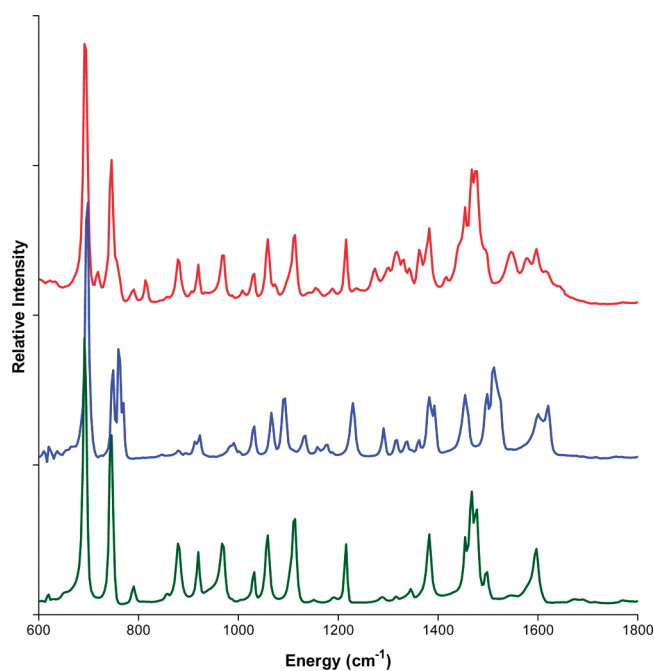


Figure 8. Infrared absorption spectra in the fingerprint region of benzylammonium chloride (green trace), (*R*)- α -methylbenzylammonium chloride (blue trace) and their 1:1 cocrystal product (red trace).

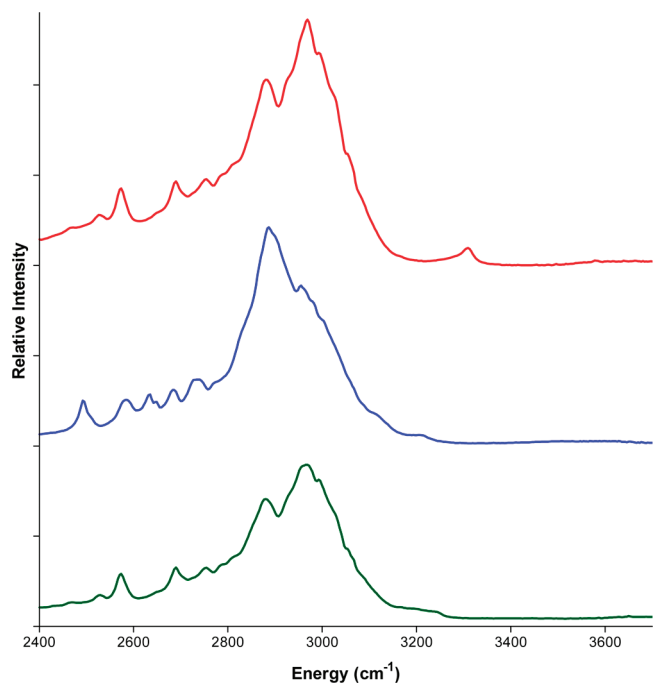


Figure 9. Infrared absorption spectra in the high-frequency region of benzylammonium chloride (green trace), (*R*)- α -methylbenzylammonium chloride (blue trace), and their 1:1 cocrystal product (red trace).

interaction of (*R*)- α -methylbenzylamine with benzylammonium chloride.

The DSC thermogram of the mixed (*R*)mBZA-Cl-BZA salt-cocrystal product was found to be more complicated than any of the other salt-cocrystal products. Whereas the other salt-cocrystal products were obtained as nonsolvates, the mixed salt-cocrystal

Table 5. Assignments of Key Absorption Bands in the Infrared Absorption Spectra of the Benzylamine–Benzylammonium Chloride, the (*R*)- α -Methylbenzylamine–(*S*)- α -Methylbenzylammonium Chloride, and the (*R*)- α -Methylbenzylamine–Benzylammonium Chloride Salt-Cocrystal Products

vibrational mode assignment	BZA-Cl-BZA salt-cocrystal	(<i>R</i>)mBZA-Cl-BZA salt-cocrystal	(<i>R</i>)mBZA-Cl-(<i>S</i>)mBZA salt-cocrystal
NH ₃ ⁺ out-of-plane bending mode	879	879	895
NH ₂ rocking mode	1144	1155	1151
NH ₂ rocking mode	1283	1273	obscured by CH ₃ deformation mode
NH ₃ ⁺ rocking mode	1331	1317	1315
NH ₃ ⁺ symmetric bending mode	1628	1616	1610
symmetric NH ₃ ⁺ stretch	3290	3309	3292

product was obtained in the form of a methanol solvate. The DSC thermogram of the mixed salt-cocrystal product contained a large desolvation transition having a temperature maximum of 64 °C (enthalpy of desolvation equal to 96 J/g). The desolvated product exhibited two additional endothermic transitions, one at a temperature of 138 °C (enthalpy equal to 22 J/g) and the other at 193 °C (enthalpy equal to 15 J/g). No changes in baseline character were noted for either transition, ruling out the possibility that either transition was associated with an endothermic decomposition.

Using an isothermal heating process, the total volatile content of the solvated benzylamine–(*R*)- α -methylbenzylammonium chloride salt-cocrystal product was determined to be 11%. The theoretical methanol content for a 1:1 stoichiometric solvate of the mixed salt-cocrystal product was calculated to be 10.8%, establishing that this product was obtained in the form of a monomethanol solvate.

The infrared absorption spectrum of the benzylamine–(*R*)- α -methylbenzylammonium chloride salt-cocrystal product was found to be the same as the spectrum of the (*R*)- α -methylbenzylamine–benzylammonium chloride salt-cocrystal product, confirming the existence of a single (*R*)mBZA-Cl-BZA salt-cocrystal product. Figures 8 and 9 contrast the infrared absorption spectra in the fingerprint and the high-frequency regions, respectively, of the mixed (*R*)mBZA-Cl-BZA salt-cocrystal product with the corresponding spectra of the BZA-Cl-BZA and (*R*)mBZA-Cl-(*S*)mBZA cocrystal products. A summary of the energies of the key salt-cocrystal vibrational bands is found in Table 5, where it may be noted that the energy of the symmetric NH₃⁺ stretching mode around 3300 cm⁻¹ is most diagnostic of salt-cocrystal formation. All of the key absorption bands can be attributed to perturbed amine or ammonium group frequencies, which would be anticipated by the sharing of the chloride ion between the two phenylalkylamine groups.

CONCLUSIONS

In previous works, it was shown that salt-cocrystal products could be formed by the interaction of carboxylic acid precursors

with salts, namely, benzoic acid with benzylammonium benzoate,⁹ or benzenecarboxylic acids and their sodium salts.¹⁰ In the present work, the scope of potential salt-cocrystal products has been extended, with phenylalkylamine precursors being shown to form (in most instances) salt-cocrystal products with phenylalkylammonium chloride salts.

Of great significance is the demonstration that stereoselectivity can exist in the formation of salt-cocrystal products when the interacting species contain centers of dissymmetry. Specifically, it has been found that a salt-cocrystal product forms as long as the salt and free base are of opposite absolute configurations, and no cocrystallization takes place when the salt and free base are of the same absolute configuration.

The basic approach in these studies has been to use X-ray powder diffraction and differential scanning calorimetry investigations to initially prove (or disprove) the existence of a particular salt-cocrystal species, and then to use vibrational spectroscopy as a means to deduce additional details of the intermolecular interactions. While the previous studies indicated that the fingerprint region (600–1800 cm⁻¹) of the infrared absorption spectrum contained the most valuable information for characterization of benzenecarboxylic acid salt-cocrystals,^{9,10} the present study indicated that the high-frequency region (2400–3700 cm⁻¹) was most useful in differentiating between salts and salt-cocrystals when amine functionalities were involved. The energies of the symmetric NH₃⁺ stretching mode around 3000 cm⁻¹ were found to be of particular importance in this regard, although the energies of the NH₃⁺ out-of-plane bending mode (around 880 cm⁻¹) and the NH₃⁺ rocking mode (around 1320 cm⁻¹) also have good utility.

The appearance of additional vibrational modes not directly attributable to either constituent situation was evident in the present study of phenylalkylamine salt-cocrystals, and this represents a different situation than that of the previously reported system of benzenecarboxylic acids and their sodium salts. In the latter system, assignments for all vibrational modes in the salt-cocrystal products could be made on the basis of the assignments for the individual components.^{9,10} This would imply the vibrational modes of the components in the benzenecarboxylic acid/sodium salt systems largely retain their individual patterns of molecular motion. On the other hand, a number of vibrational modes in phenylalkylamine salt-cocrystals had no precursor in the spectra of either the free amine or the amine salt, and the existence of the modes would signify the existence of more delocalization in the vibrational patterns of this latter system.

AUTHOR INFORMATION

Corresponding Author

*E-mail: hbrittain@centerpharmphysics.com.

REFERENCES

- Schultheiss, N.; Newman, A. Pharmaceutical cocrystals and their physicochemical properties. *Cryst. Growth Des.* **2009**, *9*, 2950–2967.
- Aakeröy, C.; Salmon, D. J. Building co-crystals with molecular sense and supramolecular sensibility. *CrystEngComm* **2005**, *7*, 439–448.
- Vishweshwar, P.; McMahon, J. A.; Bis, J. A.; Zaworotko, M. J. Pharmaceutical Cocrystals. *J. Pharm. Sci.* **2006**, *95*, 499–516.
- Shan, N.; Zaworotko, M. J. The role of cocrystals in pharmaceutical science. *Drug Discovery Today* **2008**, *13*, 440–446.
- Aakeröy, C.; Champness, N. R.; Janiak, C. Recent advances in crystal engineering. *CrystEngComm* **2010**, *12*, 22–43.

- (6) Aakeröy, C.; Fasulo, M. E.; Desper, J. Cocrystal or salt: Does it really matter?. *Mol. Pharmaceutics* **2007**, *4*, 317–322.
- (7) Childs, S. L.; Stahly, G. P.; Park, A. The Salt-cocrystal continuum: the influence of crystal structure on ionization state. *Mol. Pharmaceutics* **2007**, *4*, 323–338.
- (8) Pop, M.; Sieger, P.; Cains, P. W. Tiotropium fumarate: An interesting pharmaceutical cocrystal. *J. Pharm. Sci.* **2009**, *98*, 1820–1834.
- (9) Brittain, H. G. Vibrational spectroscopic studies of cocrystals and salts. 2. The benzylamine-benzoic acid System. *Cryst. Growth Des.* **2009**, *9*, 3497–3503.
- (10) Brittain, H. G. Vibrational spectroscopic studies of cocrystals and salts. 3. Cocrystal products formed by benzenecarboxylic acids and their sodium Salts. *Cryst. Growth Des.* **2010**, *10*, 1990–2003.
- (11) Metrangolo, P.; Pilati, T.; Terraneo, G.; Biella, S.; Resnati, G. Anion coordination and anion-templated assembly under halogen bonding control. *CrystEngComm* **2009**, *11*, 1187–1196.
- (12) Szymanski, H. A. *Interpreted Infrared Spectra*; Plenum Press: New York, 1964.
- (13) Conley, R. T. *Infrared Spectroscopy*; Allyn and Bacon: Boston, 1966.
- (14) Coates, J. Interpretation of infrared spectra, a practical approach. *Encyclopedia of Analytical Chemistry*; Meyers, R. A., Ed., John Wiley & Sons: Chichester, 2000; pp 10815–10837.
- (15) Socrates, G. *Infrared and Raman Characteristic Group Frequencies*; 3rd ed.; John Wiley & Sons: Chichester, 2001.
- (16) Bellamy, L. J.; Williams, R. L. The NH stretching frequencies of primary amines. *Spectrochim. Acta* **1957**, *9*, 341–345.
- (17) Moritz, A. G. The N–H stretching frequencies and molecular configurations of some aromatic amines. *Spectrochim. Acta* **1960**, *16*, 1176–1183.
- (18) Moritz, A. G. Intramolecular hydrogen bonds formed by primary aromatic amines. The N–H and N–D stretching frequencies of mono- and di-deuterated amines. *Spectrochim. Acta* **1962**, *18*, 671–679.
- (19) Leysen, R.; van Rysselberge, J. Study of the infrared spectra of α -substituted benzylamines. *Spectrochim. Acta* **1963**, *19*, 243–254.
- (20) Leysen, R.; van Rysselberge, J. Study of the infrared spectra of para-substituted α -alkyl-benzylamines. *Spectrochim. Acta* **1964**, *20*, 977–982.
- (21) Sacher, E. The correlation of N–H_n i.r. frequencies in amines. *Spectrochim. Acta* **1987**, *A43*, 747–751.
- (22) Borisenko, V. E.; Baturin, A. V.; Przeslawska, M.; Koll, A. Calculations of the –NH₂ group vibrations and intensities in aromatic amines by classical VFF and quantum chemical methods. *J. Mol. Struct.* **1997**, *407*, 53–62.
- (23) Castro, J. L.; López Ramírez, M. R.; López Tocón, I.; Otero, J. C. Vibrational spectra of phenylacetate and phenylglycinate Ions. *J. Mol. Struct.* **2003**, *651–653*, 601–606.
- (24) Kolev, T. Influence of intermolecular hydrogen bonding on IR-spectroscopic properties of (R)-(-)-1-phenylglycinium hydrogen squarate monohydrate in solid-state. IR-LD, Raman spectroscopy and theoretical study. *J. Mol. Struct.* **2007**, *846*, 139–146.
- (25) Ivanova, B.; Spitteller, M. Salts of aromatic amines: Crystal structures, spectroscopic and non-linear optical properties. *Spectrochim. Acta* **2010**, *A77*, 849–855.